

A reduction in marine primary productivity driven by rapid warming over the tropical Indian Ocean

Mathew Koll Roxy¹, Aditi Modi¹, Raghu Murtugudde², VinuValsala¹, SwapnaPanickal¹, S. Prasanna Kumar³, M. Ravichandran^{4,5}, Marcello Vichi⁶ and Marina Lévy⁷

¹*Centre for Climate Change Research, Indian Institute of Tropical Meteorology, Pune, India*

²*University of Maryland, College Park, Maryland, USA*

³*CSIR-National Institute of Oceanography, Goa, India*

⁴*Indian National Centre for Ocean Information Services, Hyderabad, India*

⁵*National Centre for Antarctic and Ocean Research, Goa, India*

⁶*University of Cape Town, Cape Town, South Africa*

⁷*Sorbonne Université (UPMC, Paris 6/CNRS/IRD/MNHN), LOCEAN-IPSL, Paris, France*

Corresponding author address: RoxyM. K., Indian Institute of Tropical Meteorology, Pune 411008, India. E-mail: roxy@tropmet.res.in

Abstract

Among the tropical oceans, the western Indian Ocean hosts one of the largest concentrations of marine phytoplankton blooms in summer. Interestingly, this is also the region with the largest warming trend in sea surface temperatures in the tropics during the past century—though the contribution of such a large warming to productivity changes have remained ambiguous. Earlier studies had described the western Indian Ocean as a region with the largest increase in phytoplankton during the recent decades. On the contrary, the current study points out an alarming decrease of up to 20% in phytoplankton in this region over the past six decades. We find that these trends in chlorophyll are driven by enhanced ocean stratification due to rapid warming in the Indian Ocean, which suppresses nutrient mixing from subsurface layers. Future climate projections suggest that the Indian Ocean will continue to warm, driving this productive region into an ecological desert.

Keywords

Indian Ocean warming, marine phytoplankton, chlorophyll trends, ocean stratification, Arabian Sea, climate projections

Index Terms

1605 Abrupt/rapid climate change, 1615 Biogeochemical cycles, processes, and modeling, 1616 Climate variability, 4273 Physical and biogeochemical interactions, 9340 Indian Ocean

Key Points

- Reduction of up to 20% in marine phytoplankton in the Indian Ocean during the past six decades
 - Reduction in marine productivity is attributed to the rapid warming in the Indian Ocean
 - Future climate projections indicate further warming and subsequent reduction in marine productivity
-

1. Introduction

Marine phytoplankton plays a central role in global biogeochemical cycles [Field *et al.*, 1998], forms the base of the marine food web [Chassot *et al.*, 2010], and regulates the global climate [Murtugudde *et al.*, 2002; Sabine *et al.*, 2004]. Among the tropical oceans, the western Indian Ocean hosts one of the largest concentration of phytoplankton blooms in summer [Figure 1a; Naqvi *et al.*, 2003; Prasanna Kumar *et al.*, 2001; Ryther and Menzel, 1965; Wiggert *et al.*, 2005], supporting the second largest share of the most economically valuable tuna catch [Lee *et al.*, 2005]. The monsoonal wind forcing is the strongest in the western Indian Ocean and leads to a strong coastal and open ocean upwelling resulting from coastal divergence of Ekman transport and from Ekman pumping, supplying nutrients to the surface and supporting elevated rates of primary productivity [Lévy *et al.*, 2007; McCreary *et al.*, 2009; Prasanna Kumar *et al.*, 2001; Resplandy *et al.*, 2011; Wiggert *et al.*, 2005]. Interestingly, this is also the region with the largest long-term (~100 years) trend in sea surface temperatures (SST) in the tropics [Figure 1b; Roxy *et al.*, 2014; Roxy *et al.*, 2015a]—though the contribution of such a large trend in SST to productivity changes have remained ambiguous [Behrenfeld *et al.*, 2006; Goes *et al.*, 2005; Gregg and Rousseaux, 2014; Gregg *et al.*, 2005; Prasanna Kumar *et al.*, 2010]. This ambiguity has been due to the fact that the phytoplankton trend in the Indian Ocean has been estimated from a relatively short time-series of observations over which the monsoon winds—a physical parameter which has a complex seasonality [Boyce *et al.*, 2010]—also exhibit interannual changes and trends [Goes *et al.*, 2005; Roxy *et al.*, 2015b].

Rising sea surface temperatures (SST) can enhance near-surface stratification inhibiting vertical mixing, a critical process for introducing nutrients into the euphotic zone where sufficient light is available for photosynthesis [Behrenfeld *et al.*, 2006]. This inhibits primary production and cascades through the entire food web in the region. Though Behrenfeld *et al.* [2006] indicate a reduction in net primary productivity (NPP) over most of the tropics as a result of surface thermal stratification, their results suggest an increase in NPP with respect to the rising SSTs over the western Indian Ocean from 1998 to 2004. Other studies [Goes *et al.*, 2005; Gregg *et al.*, 2005] arrive at similar results over the same period, indicating that the western Indian Ocean underwent the second largest increase in chlorophyll concentrations (indicator of phytoplankton biomass) among the open ocean regions. Goes *et al.* [2005] reported an increase of up to 350% in marine phytoplankton in this basin, and attributed this to a strengthening of summer monsoon winds in the western Indian Ocean. The relatively short time series used in these previous studies put these results at a blind spot because

long-term data is indispensable for the attribution of changes in phytoplankton to ocean warming [Beaulieu *et al.*, 2013; Henson *et al.*, 2010; Patara *et al.*, 2012a].

It is however imperative to have a firm understanding of the trends in productivity in this highly productive ocean basin, especially since it has been experiencing one of the largest warming trends over the tropical oceans. Any trend in primary production in this region can have greater implications for ecosystem processes, and biogeochemical cycling. It is also likely that such changes feed back to the ocean-atmosphere dynamics, potentially modulating the ocean circulation on longer time scales [Murtugudde *et al.*, 2002; Patara *et al.*, 2012b]. Changes in plankton production can have immense impact on marine species as well as humans [Colwell, 1996; Harvell *et al.*, 1999]. Downward trends in primary production over these upwelling areas can be detrimental to the marine food webs and the fishing industry. Data from the Food and Agriculture Organization of the United Nations (FAO) show that the Indian Ocean accounts for 20% of the total tuna catch, especially the most economically valuable bigeye tuna, making it the 2nd largest supplier to world markets. Large-scale distribution of these dominant species of tunas are associated with the phytoplankton availability and abundance [Lee *et al.*, 2005]. The need to understand the long-term trends in phytoplankton blooms in response to the rising temperatures can hardly be overemphasized.

2. Data and Methods

The recently available, quality controlled chlorophyll data blended from multiple satellite sensors (SeaWiFS, MODIS, and MERIS) bring the number of years of continuous data up to 16 years, bringing it close to the time required to extract trends in the tropical oceans including the western Indian Ocean [Beaulieu *et al.*, 2013; Henson *et al.*, 2010]. In order to validate the robustness of the satellite data, *in-situ* data from Teledyne/Webb APEX - Argo floats deployed in the Arabian Sea are used [Ravichandran *et al.*, 2012]. See Supplementary Text S1 and Figure S1 for details on observed data and validation.

Along with the extended array of satellite data, the historical simulations of chlorophyll derived by a suite of earth system models participating in the Coupled Model Intercomparison Project (CMIP5, Table S1) [Taylor *et al.*, 2012] facilitate long-term trend analysis (> 50 years). However, many of the CMIP5 models fail to represent the spatial variability of mean chlorophyll concentrations in the Indian Ocean, particularly the western region which is a robust (coastal and open ocean) upwelling zone (Text S2 and Figures S2, S3). Hence a subset of models with pattern correlation coefficients (PCC) above 0.4 (Table S1), which reasonably represent the spatial variability of chlorophyll in the Indian Ocean are selected for examining the trends. This subset of models is used for preparing an

ensemble mean of the chlorophyll trends. However, among the selected subset of models, many do not exhibit an interannual variability comparable to observations (Figure S4). This will be a limitation as the response to climate variability will be weak in these models. Hence, based on interannual variability (standard deviations) and PCC, we have selected a single model to examine the biophysical response to increased warming, the MPI-ESM-MR.

MPI-ESM-MR simulates the mean climatology of chlorophyll concentrations with a relatively lower bias and realistic spatial distribution in the Indian Ocean, particularly in the Arabian Sea where the primary production as well as the surface warming is most prominent. This model is also found to be skillful in simulating the mean state of the physical variables including SST and winds in the Indian Ocean [Prasanna, 2015], which are crucial in driving the chlorophyll variability on both interannual and long-term climate time scales in this monsoon driven basin (Figure S5). See Text S2 and Figures S2-S5 for more details on model validation and selection. It is however to be cautioned that CMIP5 historical simulations are forced with the historical changes in greenhouse gas mixing ratios and aerosol concentrations, and represent the response to increasing temperatures alone, but will not have coincident interannual variability. CMIP5 simulations can hence be compared for climatologies and trends but not for year-to-year variations.

In order to further delineate the causal role of SST warming on the chlorophyll concentrations, a sensitivity experiment using an earth system model with interactive biogeochemistry [IITM-ESM, Swapna *et al.*, 2014] is performed. In the sensitivity experiment, positive SST anomalies similar to those in the observed SST trends were added to the Indian Ocean and the biophysical response is evaluated [see Text S3 for details].

3. Results

A spatial distribution of the chlorophyll trends computed from the observations and the historical simulations indicate negative trends in the western Indian Ocean (Figure 2). Interestingly, the extremes in the observed chlorophyll trends also follow the large scale spatial distribution of the observed trends in SST, with a significant reduction in chlorophyll in the western Indian Ocean where the warming is large, and a slight increase in values in the southeastern Indian Ocean where the surface warming is suppressed. This indicates that the dynamical processes driving the SST trends must also be affecting the primary production. It may appear that the largest negative trends in chlorophyll are not at the exact locations where the largest trends in SST occur. This is not unexpected, as the largest changes in chlorophyll (Figure 2) are over regions where the mean values are also large (Figure 1a). Figure 2a shows a mean decrease of up to 30% in the observations ($P <$

0.05). The MPI-ESM-MR and ensemble mean historical simulations indicate negative trends, similar to observations, and suggest a reduction of 20% ($P < 0.05$) during the past five decades (Figure 2c, e).

The MPI-ESM-MR simulations are further employed for an extended analysis on long-term trends in chlorophyll and related physical entities. Time series of chlorophyll, SST, static stability and wind speed anomalies are computed for the region (50-65°E, 5-25°N, inset box in Figure 2) where the trends in chlorophyll concentrations are the largest. SST and chlorophyll anomalies during the past several decades exhibit a significant trend, and a strong correlation between these two variables ($r = -0.9$ in observations and $r = -0.7$ in MPI-ESM-MR, $P < 0.05$), indicating the larger role of SST trends in the Indian Ocean being detrimental to marine primary production (Figure 3a, b). Rising surface temperatures can reduce chlorophyll because they are an indication of increased surface stratification and hence suppressed vertical mixing of nutrient-rich subsurface waters [Behrenfeld *et al.*, 2006]. Density difference between the surface and subsurface layers provides a useful measure of stratification, and can be represented by the static stability parameter [Behrenfeld *et al.*, 2006; Dave and Lozier, 2013; Pond and Pickard, 1983] (Text S1). Summer mean anomalies of the static stability exhibit increasing trends indicating enhanced stratification of the western Indian Ocean under rising surface temperatures ($r = 0.75$ in observations and $r = 0.9$ in MPI-ESM-MR, Figure 3c, d). Further, the stratification is strongly correlated with the changes in chlorophyll ($r = -0.8$ in observations and $r = -0.62$ in MPI-ESM-MR, Figure 3e, f). These results clearly link the rising Indian Ocean SSTs to increased stratification and subsequent reduction in marine primary productivity over the region, during the past half century.

It is also possible that a changing monsoon circulation and winds [Roxy *et al.*, 2015b] affect the chlorophyll variability by influencing the upwelling dynamics over the region [Goes *et al.*, 2005]. An examination of the wind speed anomalies over the western Indian Ocean indicates a relatively weak correlation with the chlorophyll anomalies (Figure 3g, h). Also, the long-term change over the same region is only about 0.2 m s^{-1} (Figure 3h), which is minor compared to an SST trend of 0.6°C during the same period (Figure 3b). The wind stress curl anomalies do not show any significant trends (Figure 3i, j), indicating that trends in the wind induced upwelling and associated changes in chlorophyll are trivial during this period. In fact, the results indicate a strengthening of winds in the recent decade, which should have favored an increase in the nutrients and chlorophyll, but the correlation during this period is negative. It is obvious that increasing SSTs are playing a larger role

than the changing winds, contrary to what earlier studies have proposed, albeit for relatively shorter term records [*Goes et al.*, 2005; *Gregg et al.*, 2005].

The MPI-ESM-MR historical simulations also provides estimates of available nutrients, which can be used to investigate whether the nutrients are indeed decreasing as a result of reduced mixing due to warmer surface waters. Trend analysis of nitrate, phosphate and silicate concentrations indicate that the nutrient availability has reduced in the western Indian Ocean and around the southern tip of Indian peninsula, regions where the chlorophyll concentrations have also gone down (Figure 4). At the same time, there is an increase in nutrient availability and chlorophyll concentrations in the southeastern Indian Ocean where the corresponding SSTs show suppressed surface warming. The anomalous increase of chlorophyll in this region may be due to the decreasing stratification (Figure 4b) driven by faster rates of warming in the subsurface relative to the surface [*Dave and Lozier*, 2013].

To further delineate the causal role of the Indian Ocean warming on chlorophyll variability, model sensitivity experiments were carried out using an earth system model with an interactive ocean biogeochemistry [*Swapna et al.*, 2014] (Text S3 and Figure S6). On a large spatial scale, the results are similar to the changes observed in the MPI-ESM-MR historical simulations. Clearly, the enhanced warming has resulted in weakened nutrient mixing and a reduction of chlorophyll concentrations over most of the Arabian Sea, affirming the conclusions drawn above from observations and a CMIP5 model.

4. Discussion

Earlier studies on changes in chlorophyll had described the western Indian Ocean as among the open ocean regions with the largest increase in marine phytoplankton, but based on relatively short-term records. In the recent decades, the coastal winds over this region have strengthened and ideally, this should enhance the nutrient mixing and phytoplankton blooms. On the contrary, the current study using quality controlled blended chlorophyll data and earth system model simulations, points out an alarming decrease of up to 20% in marine phytoplankton in this region over the past six decades. We find that these trends in chlorophyll are driven by enhanced ocean stratification due to the rapid warming in the Indian Ocean, which suppresses nutrient mixing from subsurface layers.

While the current study demonstrates a decreasing trend in chlorophyll (during 1998-2013), why did the earlier studies [e.g., *Goes et al.*, 2005] indicate an increasing trend in the chlorophyll concentrations (during 1998-2005)? On a closer inspection, the time series in Fig.3 indeed shows a

slight increase in chlorophyll during 1998-2005. This trend is dominated by the changes during the years 1998-1999 which saw large ENSO variability—which has a strong association with the SST anomalies in the western Indian Ocean [Yu and Rienecker, 1999; Murtugudde et al., 2000]. Specifically, 1998 was a strong El Niño year which warmed up the western Indian Ocean, immediately followed by La Niña conditions in the year 1999 which cooled the region. This can be observed as a large dip in SST from 1998-1999, perfectly matched with an increase in the chlorophyll anomalies during this period [Murtugudde et al., 1999]. If 1998-1999 is treated as an outlier, the entire time series indicates a secular trend of decreasing chlorophyll concentrations. Apart from this, a major difference with Goes et al. [2005] is that their study considers only the coastal region of the western Arabian Sea (47-55°E, 5-10°N), where the biophysical processes are dominated by strong coastal dynamics, entrainment, advection and river runoff [Vialard et al., 2011]. Meanwhile, the current study employs a much larger region (50-65°E, 5-25°N) including the open basin where coastal processes are less of a player but the large scale monsoon forcing is dominant and the effect of wind and stratification changes on chlorophyll is easier to detect.

Establishing relationships between a warming Indian Ocean and primary productivity relies heavily on the accuracy to which changes in the phytoplankton distribution can be detected. Unfortunately, the chlorophyll concentration discerned by satellites or models is only a gross indicator of a multitude of phytoplankton species which have a fairly diverse response to environmental alterations [Huisman et al., 2006]. Other than warming temperatures, plankton fluctuations may also occur due to the limiting effects of light, zooplankton grazing and viral infection [Behrenfeld, 2014]. Nevertheless, the extended satellite data and the state-of-the-art model simulations used in our study provide a quantitative and causal evaluation of the overall chlorophyll trends, and allows for a general understanding of the changes in marine primary productivity in a monotonically warming Indian Ocean.

Available data show that the tuna catch rates in the Indian Ocean have declined by 50-90% during the past five decades [Myers and Worm, 2003; Polacheck, 2006] (Figure S7). Increased industrial fisheries is a major cause for such a huge decline. However, the reduced phytoplankton may add up as a potential stress factor in the recent decades, and exploiting a resource that may be in decline can tip it over to a point of no return. Despite a long-term decline in the tuna catch rates, there is a slight increasing trend in the catch rates in the recent decades during which the chlorophyll concentrations decreased, which suggests that ecosystem responses in the food web are complex, especially when highly migratory species are involved. Careful data gathering is needed to understand the totality of

the ecosystem response to changing stratification, especially in terms of the fisheries yields and disease pressures. It is however definitive that the Indian Ocean is warming, and CMIP5 future simulations project a further decline in marine primary productivity in the coming decades [Bopp *et al.*, 2013] (Figure S8). This is a cautionary tale considering that ecosystems can extract even weak climate links [Taylor *et al.*, 2002] and human activities are providing increasingly strong climate forcing. The Indian Ocean may thus need to be monitored more closely to see if it is acting as an early indicator of physical-biological interactions in a warming world.

Acknowledgements.

The Program for Climate Model Diagnosis and Intercomparison, and the World Climate Research Programme's working Group on coupled modelling, and the Centre for Environmental Data Archival (CEDA) are acknowledged for their roles in making available the CMIP5 multi-model data sets. The IITM-ESM simulations were performed on the High Performance Computing System at the Indian Institute of Tropical Meteorology, Ministry of Earth Sciences, India, and will be available from the corresponding author on request. This is IITM Contribution #MM/PASCAL/RP/XXX under the National Monsoon Mission setup by the Ministry of Earth Sciences, Government of India; CSIR-NIO Contribution XXX and ESSO-INCOIS Contribution 236.

References

- Adachi, Y., S. Yukimoto, M. Deushi, A. Obata, H. Nakano, T. Y. Tanaka, M. Hosaka, T. Sakami, H. Yoshimura, and M. Hirabara (2013), Basic performance of a new earth system model of the Meteorological Research Institute (MRI-ESM1), *Papers in Meteorology and Geophysics*, *64*, 1-19.
- Beaulieu, C., S. A. Henson, J. L. Sarmiento, J. P. Dunne, S. C. Doney, R. Rykaczewski, and L. Bopp (2013), Factors challenging our ability to detect long-term trends in ocean chlorophyll, *Biogeosciences*, *10*, 2711–2724.
- Behrenfeld, M. J. (2014), Climate-mediated dance of the plankton, *Nature Climate Change*, *4*(10), 880-887.
- Behrenfeld, M. J., R. T. O'Malley, D. A. Siegel, C. R. McClain, J. L. Sarmiento, G. C. Feldman, A. J. Milligan, P. G. Falkowski, R. M. Letelier, and E. S. Boss (2006), Climate-driven trends in contemporary ocean productivity, *Nature*, *444*(7120), 752-755.
- Brewin, R. J., D. E. Raitsos, G. Dall'Olmo, N. Zarokanellos, T. Jackson, M.-F. Racault, E. S. Boss, S. Sathyendranath, B. H. Jones, and I. Hoteit (2015), Regional ocean-colour chlorophyll algorithms for the Red Sea, *Remote Sensing of Environment*, *165*, 64-85.
- Bopp, L., L. Resplandy, J. Orr, S. Doney, J. Dunne, M. Gehlen, P. Halloran, C. Heinze, T. Ilyina, and R. Séférian (2013), Multiple stressors of ocean ecosystems in the 21st century: projections with CMIP5 models, *Biogeosciences*, *10*(10), 6225-6245.

- Boyce, D. G., M. R. Lewis, and B. Worm (2010), Global phytoplankton decline over the past century, *Nature*, 466(7306), 591-596.
- Chassot, E., S. Bonhommeau, N. K. Dulvy, F. Mélin, R. Watson, D. Gascuel, and O. Le Pape (2010), Global marine primary production constrains fisheries catches, *Ecology Letters*, 13(4), 495-505.
- Colwell, R. R. (1996), Global climate and infectious disease: the cholera paradigm, *Science*, 274(5295), 2025-2031.
- Dave, A. C., and M. S. Lozier (2013), Examining the global record of interannual variability in stratification and marine productivity in the low-latitude and mid-latitude ocean, *Journal of Geophysical Research: Oceans*, 118(6), 3114-3127.
- Denman, K., and M. Pena (1999), A coupled 1-D biological/physical model of the northeast subarctic Pacific Ocean with iron limitation, *Deep Sea Research Part II: Topical Studies in Oceanography*, 46(11), 2877-2908.
- Dunne, J. P., A. Gnanadesikan, J. L. Sarmiento, and R. D. Slater (2010), Technical description of the prototype version (v0) of tracers of phytoplankton with allometric zooplankton (TOPAZ) ocean biogeochemical model as used in the Princeton IFMIP model, *Biogeosciences*, 7, 3593.
- Dunne, J. P., J. G. John, E. Shevliakova, R. J. Stouffer, J. P. Krasting, S. L. Malyshev, P. Milly, L. T. Sentman, A. J. Adcroft, and W. Cooke (2013), GFDL's ESM2 Global Coupled Climate–Carbon Earth System Models. Part II: Carbon System Formulation and Baseline Simulation Characteristics, *Journal of Climate*, 26(7), 2247-2267.
- Field, C. B., M. J. Behrenfeld, J. T. Randerson, and P. Falkowski (1998), Primary production of the biosphere: integrating terrestrial and oceanic components, *Science*, 281(5374), 237.
- Goes, J. I., P. G. Thoppil, H. do R Gomes, and J. T. Fasullo (2005), Warming of the Eurasian landmass is making the Arabian Sea more productive, *Science*, 308(5721), 545-547.
- Goyet, C., and A. Poisson (1989), New determination of carbonic acid dissociation constants in seawater as a function of temperature and salinity, *Deep Sea Research Part A. Oceanographic Research Papers*, 36(11), 1635-1654.
- Gregg, W. W., and C. S. Rousseaux (2014), Decadal trends in global pelagic ocean chlorophyll: A new assessment integrating multiple satellites, in situ data, and models, *Journal of Geophysical Research: Oceans*, 119(9), 5921-5933.
- Gregg, W. W., and N. W. Casey (2007), Modeling coccolithophores in the global oceans, *Deep Sea Research Part II: Topical Studies in Oceanography*, 54(5), 447-477.
- Gregg, W. W., N. W. Casey, and C. R. McClain (2005), Recent trends in global ocean chlorophyll, *Geophysical Research Letters*, 32(3).
- Harvell, C., K. Kim, J. Burkholder, R. Colwell, P. R. Epstein, D. Grimes, E. Hofmann, E. Lipp, A. Osterhaus, and R. M. Overstreet (1999), Emerging marine diseases--climate links and anthropogenic factors, *Science*, 285(5433), 1505-1510.

Henson, S. A., J. L. Sarmiento, J. P. Dunne, L. Bopp, I. D. Lima, S. C. Doney, J. John, and C. Beaulieu (2010), Detection of anthropogenic climate change in satellite records of ocean chlorophyll and productivity, *Biogeosciences*, 7, 621-640.

Huisman, J., N. N. P. Thi, D. M. Karl, and B. Sommeijer (2006), Reduced mixing generates oscillations and chaos in the oceanic deep chlorophyll maximum, *Nature*, 439(7074), 322-325.

Ilyina, T., K. D. Six, J. Segschneider, E. Maier-Reimer, H. Li, and I. Núñez-Riboni (2013), Global ocean biogeochemistry model HAMOCC: Model architecture and performance as component of the MPI-Earth system model in different CMIP5 experimental realizations, *Journal of Advances in Modeling Earth Systems*, 5(2), 287-315.

Lee, P.-F., I.-C. Chen, and W.-N. Tzeng (2005), Spatial and temporal distribution patterns of bigeye tuna (*Thunnus obesus*) in the Indian Ocean, *ZOOLOGICAL STUDIES-TAIPEI*, 44(2), 260.

Lévy, M., D. Shankar, J. M. André, S. Sheno, F. Durand, and C. de Boyer Montegut (2007), Basin-wide seasonal evolution of the Indian Ocean's phytoplankton blooms, *Journal of Geophysical Research: Oceans (1978–2012)*, 112(C12).

Maier-Reimer, E., and K. Hasselmann (1987), Transport and storage of CO₂ in the ocean—an inorganic ocean-circulation carbon cycle model, *Climate dynamics*, 2(2), 63-90.

McCreary, J., R. Murtugudde, J. Vialard, P. Vinayachandran, J. D. Wiggert, R. R. Hood, D. Shankar, and S. Shetye (2009), Biophysical processes in the Indian Ocean, *Indian Ocean Biogeochemical Processes and Ecological Variability*, 9-32.

Moore, J. K., S. C. Doney, and K. Lindsay (2004), Upper ocean ecosystem dynamics and iron cycling in a global three-dimensional model, *Global Biogeochemical Cycles*, 18(4).

Murtugudde, R., J. Beauchamp, C. R. McClain, M. Lewis, and A. J. Busalacchi (2002), Effects of penetrative radiation on the upper tropical ocean circulation, *Journal of Climate*, 15(5), 470-486.

Murtugudde, R., J. P. McCreary, and A. J. Busalacchi (2000), Oceanic processes associated with anomalous events in the Indian Ocean with relevance to 1997–1998, *Journal of Geophysical Research: Oceans (1978–2012)*, 105(C2), 3295-3306.

Murtugudde, R. G., S. R. Signorini, J. R. Christian, A. J. Busalacchi, C. R. McClain, and J. Picaut (1999), Ocean color variability of the tropical Indo-Pacific basin observed by SeaWiFS during 1997–1998, *Journal of Geophysical Research*, 104(C8), 18351-18318,18366.

Müller, D., H. Krasemann, R. J. Brewin, C. Brockmann, P.-Y. Deschamps, R. Doerffer, N. Fomferra, B. A. Franz, M. G. Grant, and S. B. Groom (2015), The Ocean Colour Climate Change Initiative: I. A methodology for assessing atmospheric correction processors based on in-situ measurements, *Remote Sensing of Environment*, 162, 242-256.

Myers, R. A., and B. Worm (2003), Rapid worldwide depletion of predatory fish communities, *Nature*, 423(6937), 280-283.

Naqvi, S., H. Naik, and P. Narvekar (2003), The Arabian Sea, in *Biogeochemistry*, edited by K. Black and G. Shimmield, pp. 156–206, Blackwell, Oxford.

- Narvekar, J., and S. Prasanna Kumar (2014), Mixed layer variability and chlorophyll a biomass in the Bay of Bengal, *Biogeosciences*, *11*, 3819-3843.
- Oschlies, A. (2001), Model-derived estimates of new production: New results point towards lower values, *Deep Sea Research Part II: Topical Studies in Oceanography*, *48*(10), 2173-2197.
- Palmer, J., and I. Totterdell (2001), Production and export in a global ocean ecosystem model, *Deep Sea Research Part I: Oceanographic Research Papers*, *48*(5), 1169-1198.
- Patara, L., M. Vichi, and S. Masina (2012a), Impacts of natural and anthropogenic climate variations on North Pacific plankton in an Earth System Model, *Ecological modelling*, *244*, 132-147.
- Patara, L., M. Vichi, S. Masina, P. G. Fogli, and E. Manzini (2012b), Global response to solar radiation absorbed by phytoplankton in a coupled climate model, *Climate dynamics*, *39*(7-8), 1951-1968.
- Polacheck, T. (2006), Tuna longline catch rates in the Indian Ocean: Did industrial fishing result in a 90% rapid decline in the abundance of large predatory species?, *Marine Policy*, *30*(5), 470-482.
- Pond, S., and G. L. Pickard (1983), *Introductory dynamical oceanography*, 241 pp., Pergamon Press, New York.
- Prasanna Kumar, S., P. R. Roshin, J. Narvekar, P. Dinesh Kumar, and E. Vivekanandan (2010), What drives the increased phytoplankton biomass in the Arabian Sea?, *Current Science*, *99*(1), 101-106.
- Prasanna Kumar, S., M. Madhupratap, M. Dileepkumar, P. Muraleedharan, S. DeSouza, M. Gauns, and V. Sarma (2001), High biological productivity in the central Arabian Sea during the summer monsoon driven by Ekman pumping and lateral advection, *Current Science*, *81*(12), 1633-1638pp.
- Prasanna, V. (2015), Assessment of South Asian Summer Monsoon Simulation in CMIP5-Coupled Climate Models During the Historical Period (1850–2005), *Pure and Applied Geophysics*, 1-24.
- Ravichandran, M., M. Girishkumar, and S. Riser (2012), Observed variability of chlorophyll-a using Argo profiling floats in the southeastern Arabian Sea, *Deep Sea Research Part I: Oceanographic Research Papers*, *65*, 15-25.
- Resplandy, L., M. Lévy, G. Madec, S. Pous, O. Aumont, and D. Kumar (2011), Contribution of mesoscale processes to nutrient budgets in the Arabian Sea, *Journal of Geophysical Research: Oceans (1978–2012)*, *116*(C11).
- Roxy, M. K., K. Ritika, P. Terray, and S. Masson (2014), The curious case of Indian Ocean warming, *Journal of Climate*, *27*(22), 8501-8509.
- Roxy, M. K., K. Ritika, P. Terray, and S. Masson (2015a), Indian Ocean warming—the bigger picture, *Bull. Am. Meteorol. Soc.*, *96*(7), 1070-1071.
- Roxy, M. K., K. Ritika, P. Terray, R. Murtugudde, K. Ashok, and B. N. Goswami (2015b), Drying of Indian subcontinent by rapid Indian Ocean warming and a weakening land-sea thermal gradient, *Nature Communications*, *6*, 7423.

- Rykaczewski, R. R., and J. P. Dunne (2011), A measured look at ocean chlorophyll trends, *Nature*, 472(7342), E5-E6.
- Ryther, J. H., and C. Yentsch (1957), The estimation of phytoplankton production in the ocean from chlorophyll and light data, *Limnology and oceanography*, 281-286.
- Ryther, J., and D. Menzel (1965), On the production, composition, and distribution of organic matter in the Western Arabian Sea, *Deep Sea Research and Oceanographic Abstracts*, 12(2), 199-209.
- Sabine, C. L., R. A. Feely, N. Gruber, R. M. Key, K. Lee, J. L. Bullister, R. Wanninkhof, C. Wong, D. W. R. Wallace, and B. Tilbrook (2004), The oceanic sink for anthropogenic CO₂, *Science*, 305(5682), 367.
- Séférian, R., L. Bopp, M. Gehlen, J. C. Orr, C. Ethé, P. Cadule, O. Aumont, D. S. y Méliá, A. Voltaire, and G. Madec (2013), Skill assessment of three earth system models with common marine biogeochemistry, *Climate Dynamics*, 40(9-10), 2549-2573.
- Swapna, P., M. Roxy, K. Aparna, K. Kulkarni, A. Prajeesh, K. Ashok, R. Krishnan, S. Moorthi, A. Kumar, and B. Goswami (2014), The IITM Earth System Model: Transformation of a Seasonal Prediction Model to a Long Term Climate Model, *Bulletin of the American Meteorological Society*.
- Taylor, A. H., J. I. Allen, and P. A. Clark (2002), Extraction of a weak climatic signal by an ecosystem, *Nature*, 416(6881), 629-632.
- Taylor, K. E., R. J. Stouffer, and G. A. Meehl (2012), An Overview of CMIP5 and the Experiment Design, *Bulletin of the American Meteorological Society*, 93(4).
- Vialard, J., A. Jayakumar, C. Gnanaseelan, M. Lengaigne, D. Sengupta, and B. Goswami (2011), Processes of 30–90 days sea surface temperature variability in the northern Indian Ocean during boreal summer, *Climate Dynamics*, 38(9-10), 1901-1916.
- Vichi, M., N. Pinardi, and S. Masina (2007), A generalized model of pelagic biogeochemistry for the global ocean ecosystem. Part I: Theory, *Journal of Marine Systems*, 64(1), 89-109.
- Yu, L., and M. M. Rienecker (1999), Mechanisms for the Indian Ocean warming during the 1997–98 El Nino, *Geophysical Research Letters*, 26(6), 735-738.
- Wiggert, J., R. Hood, K. Banse, and J. Kindle (2005), Monsoon-driven biogeochemical processes in the Arabian Sea, *Progress in Oceanography*, 65(2-4), 176-213.
- Zahariev, K., J. R. Christian, and K. L. Denman (2008), Preindustrial, historical, and fertilization simulations using a global ocean carbon model with new parameterizations of iron limitation, calcification, and N₂ fixation, *Progress in Oceanography*, 77(1), 56-82.

Figure Legends

Figure 1. **a**, Climatological boreal summer (June-Sept) net primary production ($\text{mg C m}^{-2} \text{ day}^{-1}$) during 1998-2007, derived based on SeaWiFS chlorophyll, Photosynthetically Active Radiation (PAR) and AVHRR SST using the Vertically Generalized Production Model (VGPM)[*Behrenfeld et al.*, 2006]. **b**, Observed trend in summer SST ($^{\circ}\text{C}$ per 63 years) during 1950-2012, using HadISST.

Figure 2. Chlorophyll and SST trend in **(a, b)** observations, and historical simulations of **(c, d)** MPI-ESM-MR and **(e, f)** ensemble mean of selected five models, during summer. The inset box ($50\text{-}65^{\circ}\text{E}$, $5\text{-}25^{\circ}\text{N}$) indicates the region under consideration, with the largest trends in chlorophyll concentrations.

Figure 3. Mean summer anomalies of **(a, b)** chlorophyll and SST, **(c, d)** SST and static stability **(e, f)** chlorophyll and static stability, **(g, h)** chlorophyll and wind speed, **(i, j)** chlorophyll and wind stress curl in the western Indian Ocean ($50\text{-}65^{\circ}\text{E}$, $5\text{-}25^{\circ}\text{N}$, inset box in Figure 2), in observations (left) and MPI-ESM-MR historical simulations (right). Positive wind stress curl anomalies indicate upwelling. All trend lines shown are statistically significant ($P < 0.05$). Dashed line in observed chlorophyll time series indicates the period with data uncertainty (See Methods). Note that the historical simulations are forced with changes in greenhouse gases alone, and can be used for comparing climatologies and trends, but not for year-to-year variations.

Figure 4. Trends in **a**, SST ($^{\circ}\text{C}$), **b**, static stability, **c**, chlorophyll (mg m^{-3}) and **d-f**, nitrate ($\mu\text{mol L}^{-1}$), phosphate ($10^{-1} \mu\text{mol L}^{-1}$) and silicate ($\mu\text{mol L}^{-1}$) anomalies in the MPI-ESM-MR historical simulations for June-September, during 1950-2005 (56 years).

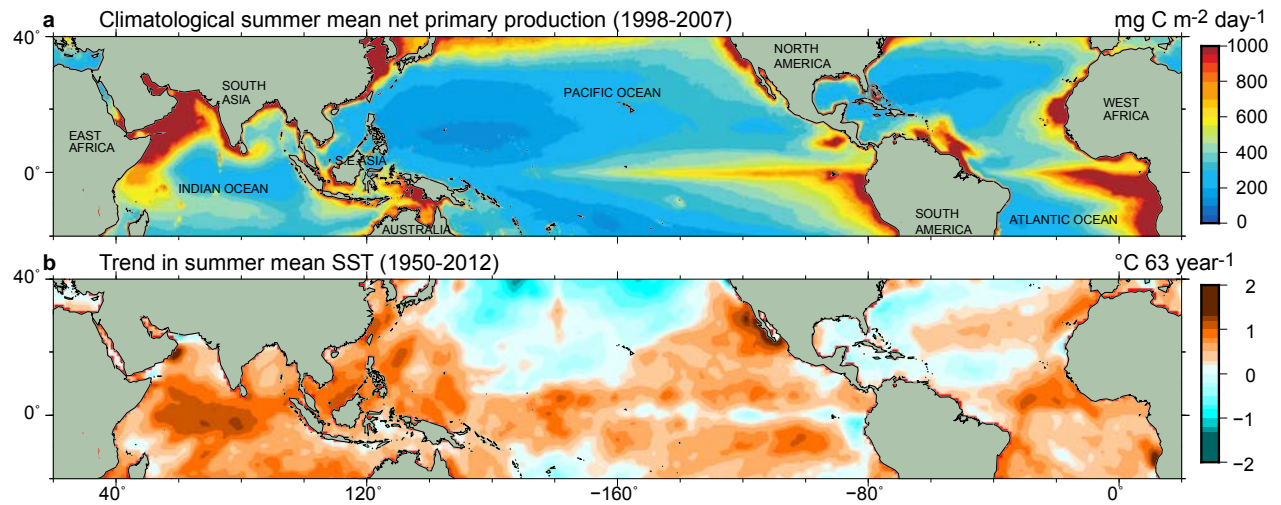


Figure 1. **a**, Climatological boreal summer (June-Sept) net primary production ($\text{mg C m}^{-2} \text{ day}^{-1}$) during 1998-2007, derived based on SeaWiFS chlorophyll, Photosynthetically Active Radiation (PAR) and AVHRR SST using the Vertically Generalized Production Model (VGPM)[Behrenfeld *et al.*, 2006]. **b**, Observed trend in summer SST ($^{\circ}\text{C}$ per 63 years) during 1950-2012, using HadISST.

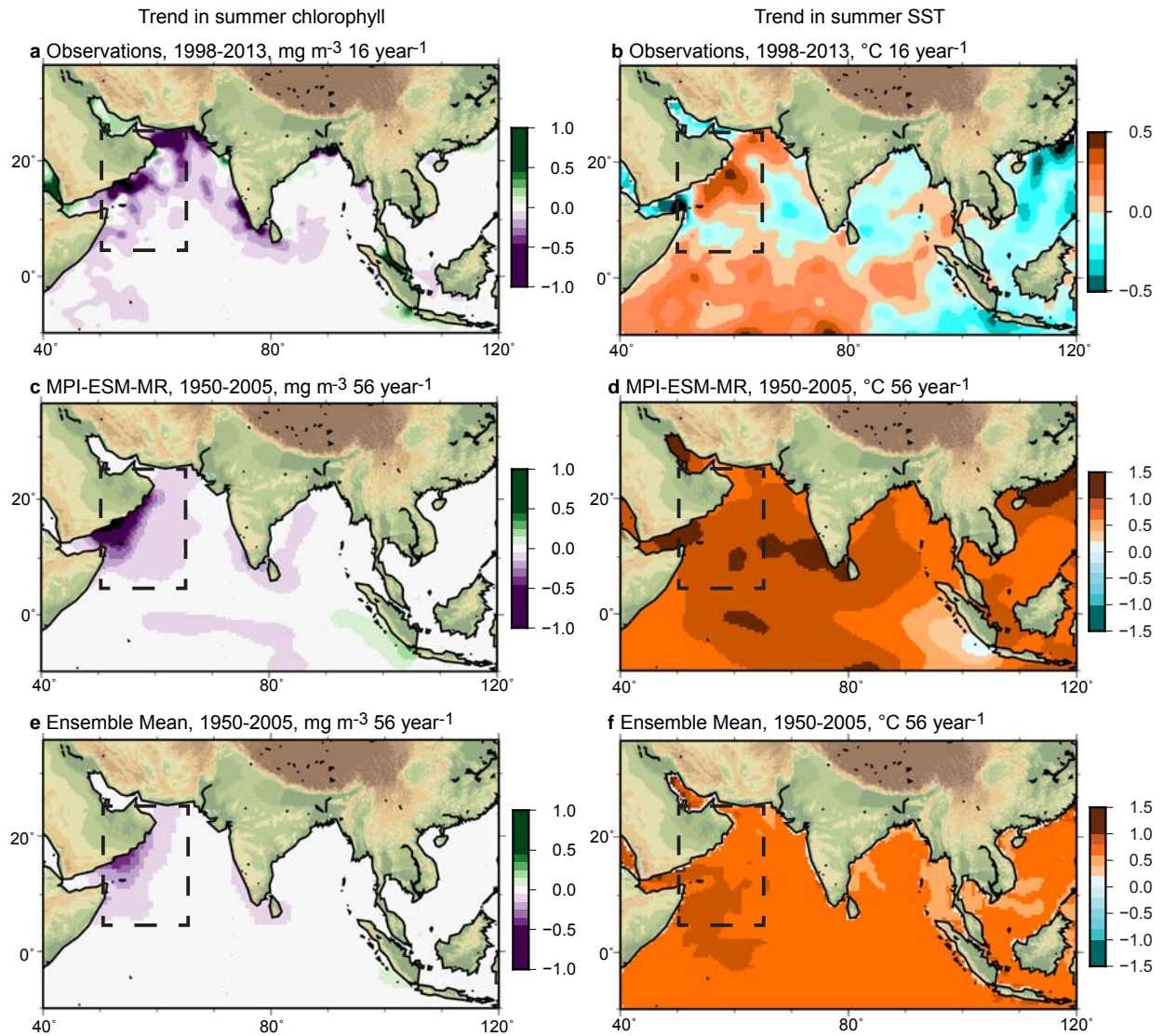


Figure2. Chlorophyll and SST trend in (a, b) observations, and historical simulations of (c, d) MPI-ESM-MR and (e, f) ensemble mean of selected five models, during summer. The inset box (50-65°E, 5-25°N) indicates the region under consideration, with the largest trends in chlorophyll concentrations.

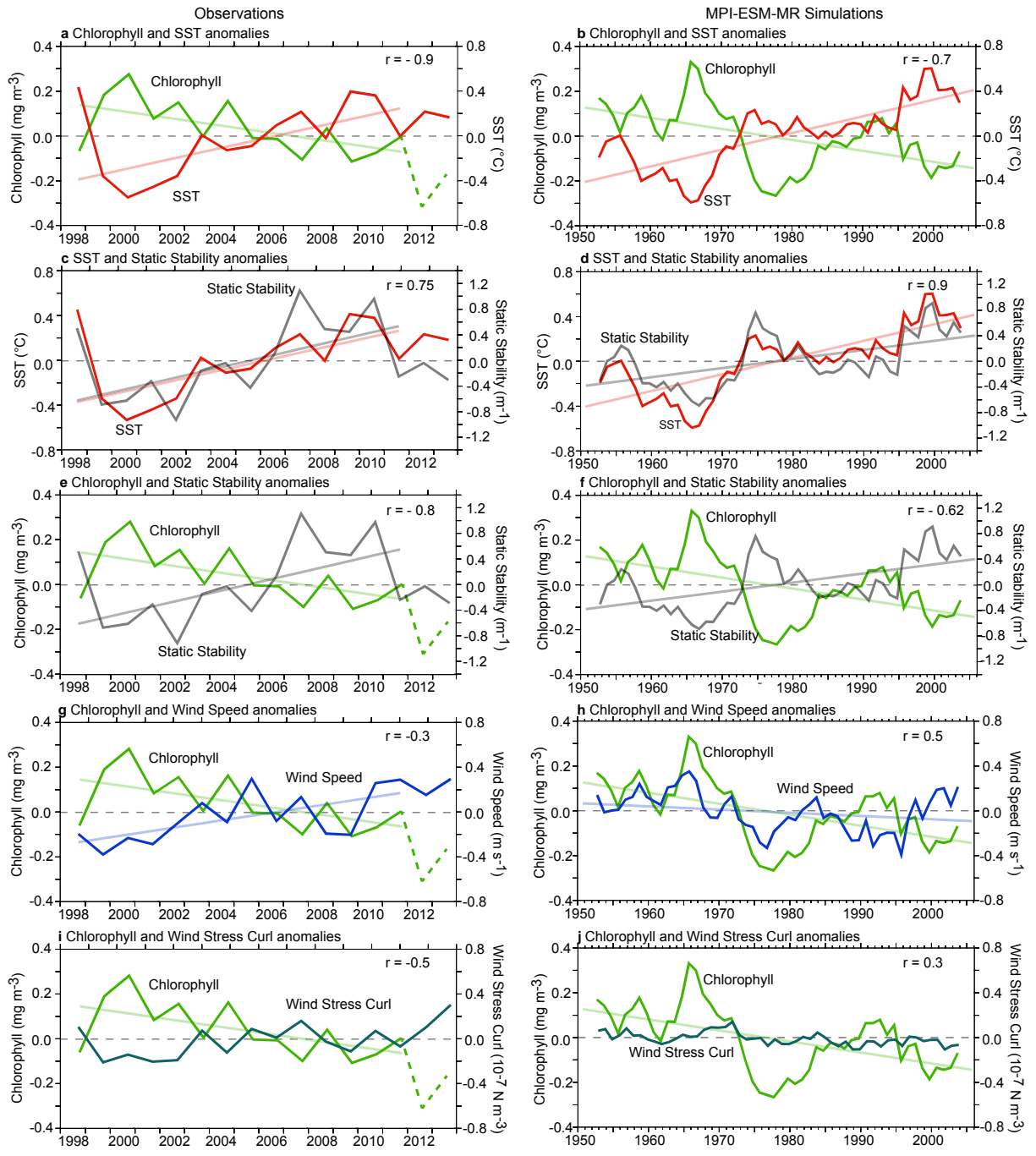


Figure 3. Mean summer anomalies of (a, b) chlorophyll and SST, (c, d) SST and static stability (e, f) chlorophyll and static stability, (g, h) chlorophyll and wind speed, (i, j) chlorophyll and wind stress curl in the western Indian Ocean (50-65°E, 5-25°N, inset box in Figure 2), in observations (left) and MPI-ESM-MR historical simulations (right). Positive wind stress curl anomalies indicate upwelling. All trend lines shown are statistically significant ($P < 0.05$). Dashed line in observed chlorophyll time series indicates the period with data uncertainty (See Methods). Note that the historical simulations are forced with changes in greenhouse gases alone, and can be used for comparing climatologies and trends, but not for year-to-year variability.

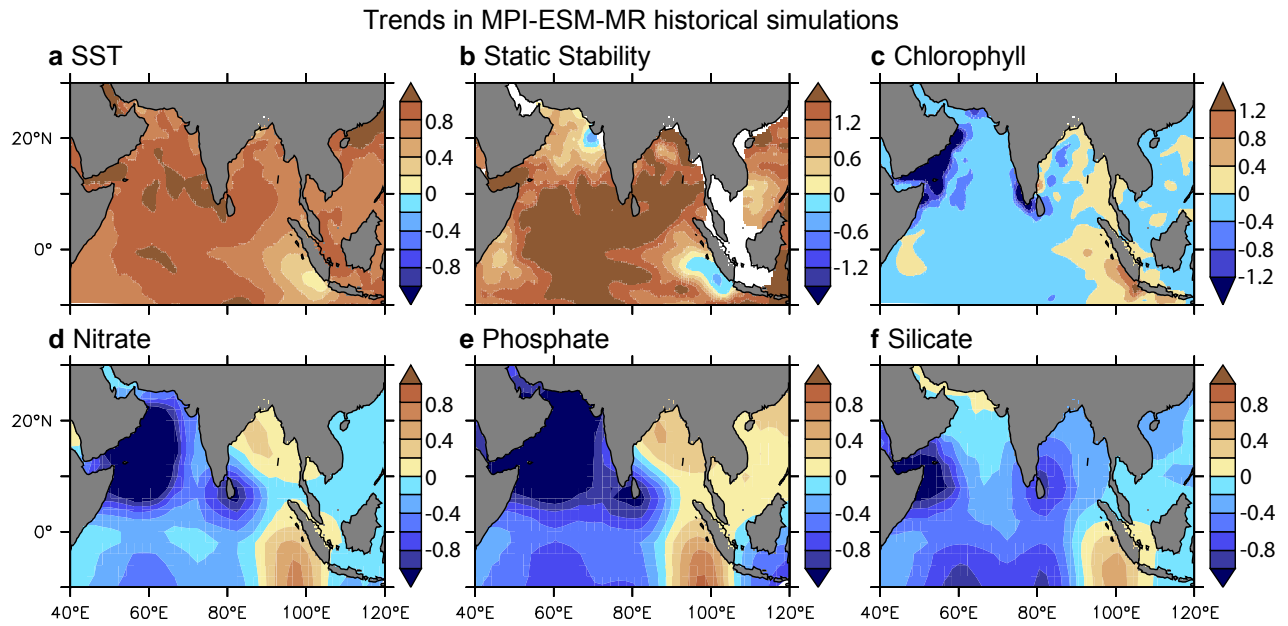


Figure4. Trends in **a**, SST ($^{\circ}\text{C}$), **b**, static stability, **c**, chlorophyll (mg m^{-3}) and **d-f**, nitrate ($\mu\text{mol L}^{-1}$), phosphate ($10^{-1} \mu\text{mol L}^{-1}$) and silicate ($\mu\text{mol L}^{-1}$) anomalies in the MPI-ESM-MR historical simulations for June-September, during 1950-2005 (56 years).

Supporting Information for

A reduction in marine primary productivity driven by rapid warming over the tropical Indian Ocean

Mathew Koll Roxy¹, Aditi Modi¹, Raghu Murtugudde², Vinu Valsala¹,
Swapna Panickal¹, S. Prasanna Kumar³, M. Ravichandran^{4,5}, Marcello Vichi⁶
and Marina Lévy⁷

¹Centre for Climate Change Research, Indian Institute of Tropical Meteorology, Pune, India, ²University of Maryland, College Park, Maryland, USA, ³CSIR-National Institute of Oceanography, Goa, India, ⁴Indian National Centre for Ocean Information Services, Hyderabad, India, ⁵National Centre for Antarctic and Ocean Research, Goa, India, ⁶University of Cape Town, Cape Town, South Africa, ⁷Sorbonne Université (UPMC, Paris 6/CNRS/IRD/MNHN), LOCEAN-IPSL, Paris, France

Contents of this file

Text S1 to S3

Figures S1 to S8

Table S1

Introduction

This supporting information provides further details on the observed data, CMIP5 historical simulations and the Earth System Model utilized in the study. It also includes additional figures validating the historical simulations with respect to observations, and the statistical techniques used. A detailed examination of the change in nutrients along with the changes in SST, stratification and chlorophyll is also provided.

Text S1.

Observed Data. Though marine primary production can be assessed directly using field flux measurements, chlorophyll pigment concentration measured through satellites is used as a convenient indicator of phytoplankton biomass and extent, as it represents the magnitude and variance in marine primary production and captures the first order changes in phytoplankton biomass [Ryther and Yentsch, 1957]. These satellite observations, which are mostly based on the visible bands of the radiance spectra (412-555 nm), lack consistent and accurate measurements of surface chlorophyll whenever cloudy conditions persist, which of course, is an integral part of the Asian summer monsoon season. Though seasonal and monthly mean composites can be derived from satellite data to some extent, it is challenging to derive robust signals of long-term trends of chlorophyll over the Indian Ocean because the current availability of satellite data is limited to a fairly short period since the satellite era [Boyce *et al.*, 2010; Rykaczewski and Dunne, 2011]. Studies suggest that the number of years required to detect a trend above the natural variability in most of the global oceans is 50-60 years, though a shorter period of 20-30 years could be used to extract the trends in the tropical oceans including the western Indian Ocean [Beaulieu *et al.*, 2013; Henson *et al.*, 2010]. The recently available satellite data blended from the multiple sensors of satellites bring the number of years of continuous data up to 16 years, bringing it close to the required trend detection time. The chlorophyll data is obtained from the European Space Agency's Ocean Color-Climate Change Initiative (OC-CCI) project [Müller *et al.*, 2015]. The OC-CCI product comprises of quality controlled chlorophyll data blended from the multiple sensors of SeaWiFS, MODIS, and MERIS satellites at 4 km-by-4 km horizontal resolution. The blended suite of chlorophyll-*a* concentration is atmospherically corrected, band shifted to SeaWiFS wavebands. The OC-CCI algorithm corrects the data for the effects of sun glint, semi-transparent clouds, and atmospheric dust aerosols, which primarily occur during monsoon. This has led to a large increase in ocean-color coverage in the OC-CCI chlorophyll data and hence permit us to resolve the climate driven trends of phytoplankton in summer months [Brewin *et al.*, 2015]. The OC-

CCI data is available for the period 1998-2013. However, the last couple of years (2012 and 2013) suffer from data gaps (less than 50% coverage) in the Arabian Sea, which could introduce spurious trends. These two years are presented in the analysis for an overview, but are not utilized for estimating the trends and correlation coefficients in the current analysis.

In order to validate the robustness of the satellite data, *in-situ* data from Teledyne/Webb APEX - Argo floats deployed in the Arabian Sea are used [Ravichandran *et al.*, 2012]. These floats were equipped with WETLabs ECO FLNTU package for measuring chlorophyll-a fluorescence (470 nm) with an accuracy of 0.02 mg m⁻³. The chlorophyll was measured from about 10 m to 2000 m depth, with a vertical resolution of about 5 m in the top 150 m. OC-CCI data is averaged over a region within the trajectories of the Argo floats (60-70°E, 5-15°N) and compared for the period during which *in-situ* data is available (year 2010). It should be taken into account that while the OC-CCI data represents satellite measurements at the sea surface, the *in-situ* data used for comparison is at about 10 m depth. Also, the *in-situ* data is measured at daily intervals, capturing fine details of the variability. Regardless of these limitations, both the time series show a high correlation ($r = 0.92$), statistically significant at 95% confidence level (Figure S1). There are slight discrepancies in the magnitude, which are probably due to the differences in the depth, frequency and location of these measurements. Nevertheless, OC-CCI captures the seasonal variability of the chlorophyll anomalies in the Indian Ocean with high fidelity, and indicates that it is useful for examining the climate driven trends in the basin.

Hydrographic data including SST and density are obtained from the Hadley Centre EN4 dataset containing Argo observations. Ocean stratification is estimated from the density difference between the surface and a depth of 200m, using a stability parameter,

$$E = -\frac{1}{\rho} \frac{\partial \rho}{\partial z}$$

where E is the static stability parameter (m⁻¹), ρ is the density (kg m⁻³) of the water and z is the depth (m) [Behrenfeld *et al.*, 2006; Narvekar and Prasanna Kumar, 2014].

Sea surface (10 m) wind speed at 0.25° grid resolution is obtained from the multi-satellite blended sea winds provided by NOAA/NCDC. Wind stress curl is estimated using

$$\nabla \times \tau = \frac{\partial \tau_y}{\partial x} - \frac{\partial \tau_x}{\partial y}$$

where τ_x and τ_y denote the eastward and northward components of wind stress. A positive wind stress curl indicates wind induced upwelling, and vice-versa.

Text S2.

CMIP5 Historical Simulations. In order to ascertain the role of a warming Indian Ocean on the long-term chlorophyll trends, a suite of historical simulations by earth system models participating in the Coupled Model Intercomparison Project (CMIP5) are used (Table S1). These historical simulations are compared with the observations for the same period (1998-2005) for their ability to reproduce the spatial distribution of mean climatology and interannual variability of chlorophyll concentrations in the Indian Ocean (Figures S2-S4). Five good models are selected based on their skills in realistic simulation of the mean and variability and pattern correlations ($r > 0.4$) over the north Indian Ocean. Ensemble means of these five models, namely the NOAA-GFDL-ESM2M, NOAA-GFDL-ESM2G, MPI-ESM-LR, MPI-ESM-MR and IPSL-CM5A-MR are used to examine the trends in the chlorophyll concentrations. Pattern correlation coefficients (PCC) computed between the summer mean chlorophyll values simulated by the models and the observations for the same period for the north Indian Ocean (50-100°E, 5-25°N) exhibits the highest correlation coefficients for the MPI-ESMs ($r > 0.5$), larger than the PCC for the ensemble mean ($r = 0.39$). This means

that the MPI-ESMs behave like the ensemble, but have a larger fidelity in representing the spatial distribution of chlorophyll variability in the Indian Ocean.

MPI-ESMs simulate the mean climatology of chlorophyll concentrations with less bias and realistic spatial distribution in the Indian Ocean, particularly in the Arabian Sea where the primary production as well as the surface warming is most prominent. However, the model has an obvious positive bias in the simulated chlorophyll concentrations in the equatorial Indian Ocean. This could be due to a model misinterpretation of the equatorial dynamics in this region—as upwelling driven by equatorial easterlies are not a robust feature of the Indian Ocean—which climate models very often fail to reproduce [McCreary *et al.*, 2009]. Among the two versions of MPI-ESMs used here, the lower-resolution (LR, $r = 0.59$) exhibits a pattern correlation higher than that of the higher-resolution (MR, $r = 0.50$). However, the higher-resolution model is chosen for further analysis as it has relatively lesser bias in most of the Indian Ocean including the equatorial regions, as well as the Bay of Bengal and western Indian Ocean (Figure S3). Also, MPI-ESM-MR features one of the highest ocean resolutions (0.4°) among all the available CMIP5 models, and the temperature biases are smaller in MR, compared to LR. Moreover, the adaptation of a more complex version of biogeochemistry model along with the higher resolution in MR can be expected to yield a more accurate simulation of chlorophyll and associated physical processes, and consequently provide a better insight into bio-physical coupling process. Hence MPI-ESM-MR is used as a representative model, based on the selected set of CMIP5 historical simulations, for extensive process study.

The MPI-ESM-MR model is found to be skillful in simulating the mean state of the physical variables including SST and winds in the Indian Ocean [Prasanna, 2015], which are crucial in driving the chlorophyll variability on both interannual and long-term climate time scales in a basin which is monsoon driven (Figure S5). Pattern correlations between the model simulations and observations yield significant correlation coefficients for SST ($r = 0.88$), winds ($r = 0.95$) and static stability ($r = 0.93$), at 95% confidence levels. The model skillfully simulates the magnitude (maximum 1.0°C and above) and spatial distribution of the observed Indian Ocean SST trends during 1950–2005, with the maximum warming spread over the west-central Indian Ocean (Arabian Sea) and minimum over the southeastern part of the basin. Historical data of chlorophyll, SST, winds and density for the period 1950–2005, simulated by MPI-ESM-MR is utilized to examine the climate driven trends in marine primary productivity.

It is however to be cautioned that CMIP5 historical simulations have some obvious limitations. Firstly, they are not hindcasts, but simulations forced with the historical changes in greenhouse gas mixing ratios (radiative forcing). CMIP5 models are typically spun up for the pre-industrial CO_2 levels and integrated forward and thus possess their own internal variability when it comes to seasonal-to-interannual and longer timescale variabilities with no correspondence to actual events such as El Niño-Southern Oscillation (ENSO) or Indian Ocean Dipole (IOD) in observations. Hence the historical simulations of chlorophyll would represent the response to increasing temperatures alone, but will not have the year-to-year variability as in observations (to be precise, coincident interannual variability). These CMIP5 simulations can hence be compared for climatologies and trends but not for year-to-year variabilities. Secondly, while the observations are of very high spatial resolution (less than 0.1° at source, 0.25° used here) and include small scale variabilities, the model historical simulations are of relatively lower resolution ($0.4^\circ\sim 0.5^\circ$) and have a low skill in resolving sub-mesoscale eddies which are prominent in these regions. This means that while the model will be able to represent trends and variabilities on a large spatial scale, it will not be able to do so for small regions.

Marine biogeochemistry in MPI-ESM is represented by the Hamburg Ocean Carbon Cycle (HAMOCC) model [Ilyina *et al.*, 2013]. HAMOCC simulates the oceanic carbon cycles along with other biogeochemical elements, and prognostically computes up to seventeen tracers in the water column. Marine biology dynamics in HAMOCC is based on an extended NPZD (nutrient, phytoplankton, zooplankton and detritus) model, which connects biogeochemical cycles and trophic levels through the uptake of nutrients and remineralization of organic matter. Phytoplankton growth in the model follows Michaelis-Menten kinetics,

and depends on temperature, light, and nutrient availability. Inorganic carbon chemistry in HAMOCC mainly follows Maier-Reimer and Hasselmann[1987] with a revised estimation of chemical constants[Goyet and Poisson, 1989]. HAMOCC also incorporates a simplified marine sulfur cycle which includes the production, bacterial consumption, photolysis, and sea-air gas exchange of dimethylsulphide.

Text S3.

IITM Earth System Model.In order to delineate the causal role of SST warming on the nutrient mixing and the chlorophyll concentrations, a sensitivity experiment using the standard configuration of an earth system model with interactive biogeochemistry, the IITM-ESM[Swapna et al., 2015] is used. The oceanic component (GFDL MOM4p1) has a 0.25–0.5° horizontal resolution, 40 vertical levels and includes an ice model. The atmospheric component (NCEP GFS) is at T126 (~0.9°)horizontal resolution and 64 sigma-pressure hybrid levels. The oceanic component is coupled with a biogeochemistry module, TOPAZ [Dunne et al., 2010]. The model exhibits reasonable skills in simulating the monsoonal characteristics over the Indian Ocean, including that of SST and chlorophyll[Swapna et al., 2015]. The coupled configuration of IITM-ESM is time integrated over a period of 50 years, and serves as the reference run (ESM_{CTL}). Ensembles (10 members) of short integrations for 10 different summer monsoon seasons(June-September) from the (ESM_{CTL})were performed by adding temperature anomalies to the SSTs in the Indian Ocean(ESM_{IO}). Positive anomalies of the order of 1.5°C was added over the region, in such a way that it tapers out by the limits of the domain (50–65°E, 5°S–10°N). The difference between ESM_{IO}and ESM_{CTL}is taken as the model chlorophyll response to the summer warming over the Indian Ocean. FigureS6 shows the model-simulated chlorophyll anomalies in response to a warming simulated over the western Indian Ocean. The response corresponds to an SST increase of about 1.0°C added to the entire Indian Ocean basin to represent the basin-wide warming, with a maximum increase of 1.5°C in the west-central region, similar to the observed trends during the northern summer.

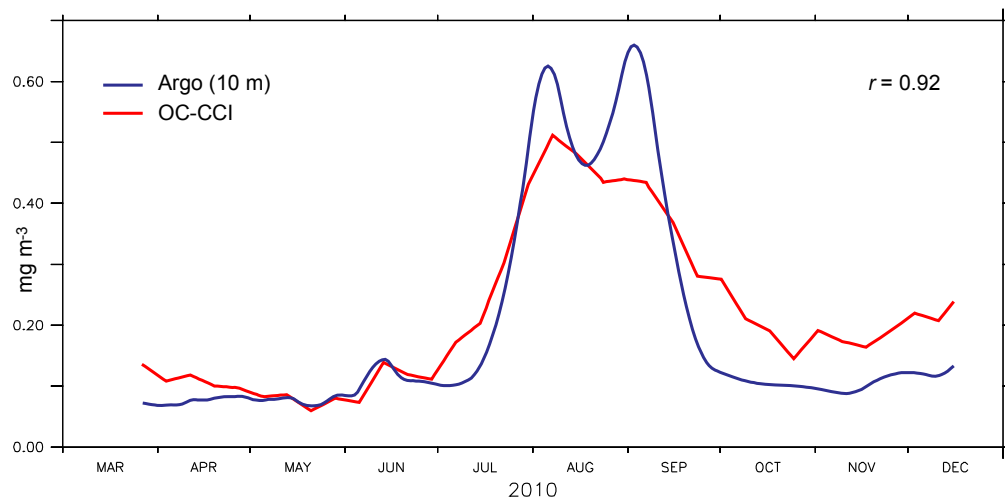


Figure S1. Temporal evolution of chlorophyll-a (mg m^{-3}) during the year 2010, derived from an Argo float at 10 m depth (blue) and OC-CCI data (red) for a region where the data points coincide in the Arabian Sea ($60\text{-}70^\circ\text{E}$, $5\text{-}15^\circ\text{N}$). The correlation coefficient ($r = 0.92$) is significant at 95% confidence level, using a standard two-tailed Student's t-test.

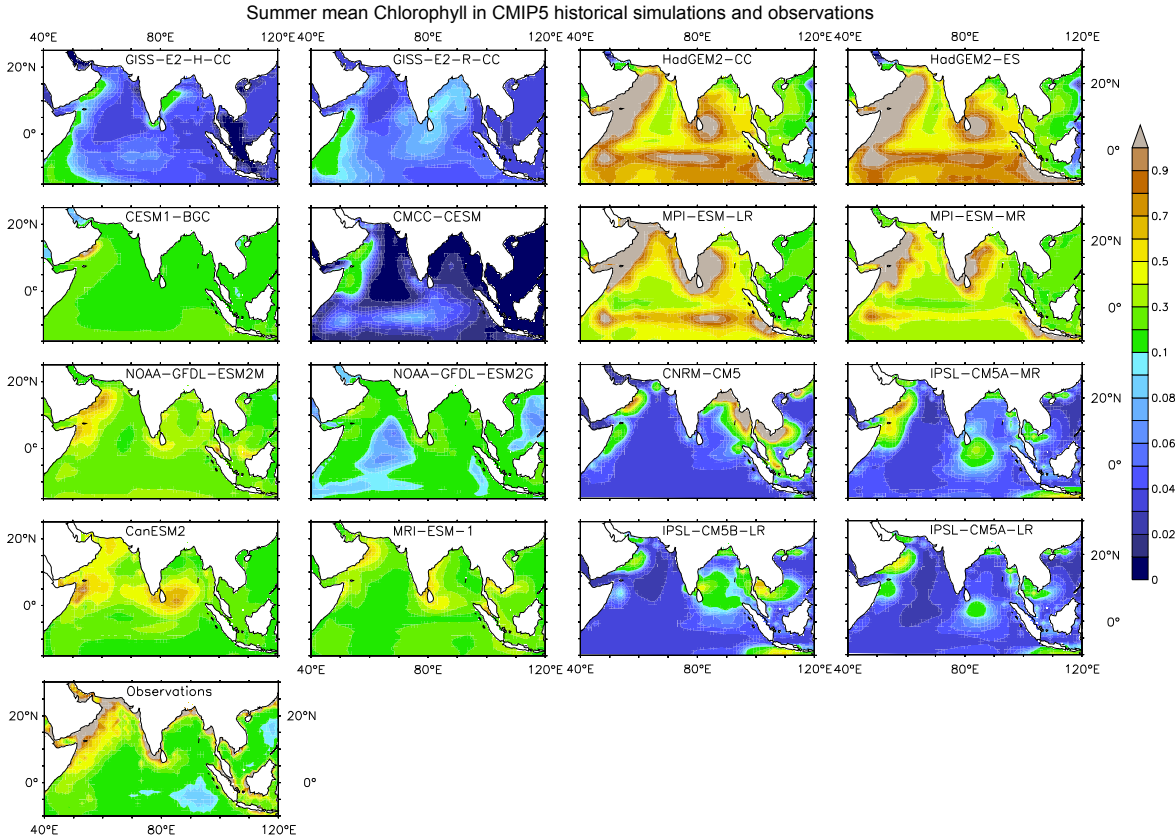


Figure S2. Climatology of June-September mean chlorophyll concentration distribution obtained from CMIP5 models and observations, for the years 1998-2005.

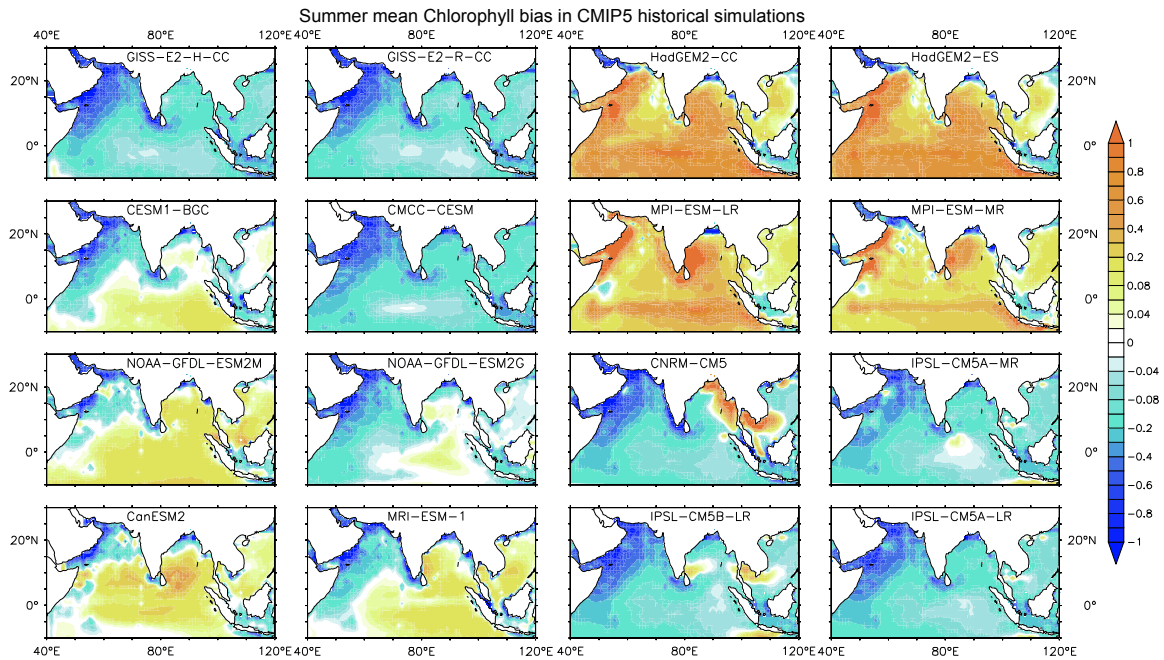


Figure S3. Bias (model – observations) in the CMIP5 simulations mean chlorophyll concentration distribution, for the years 1998-2005.

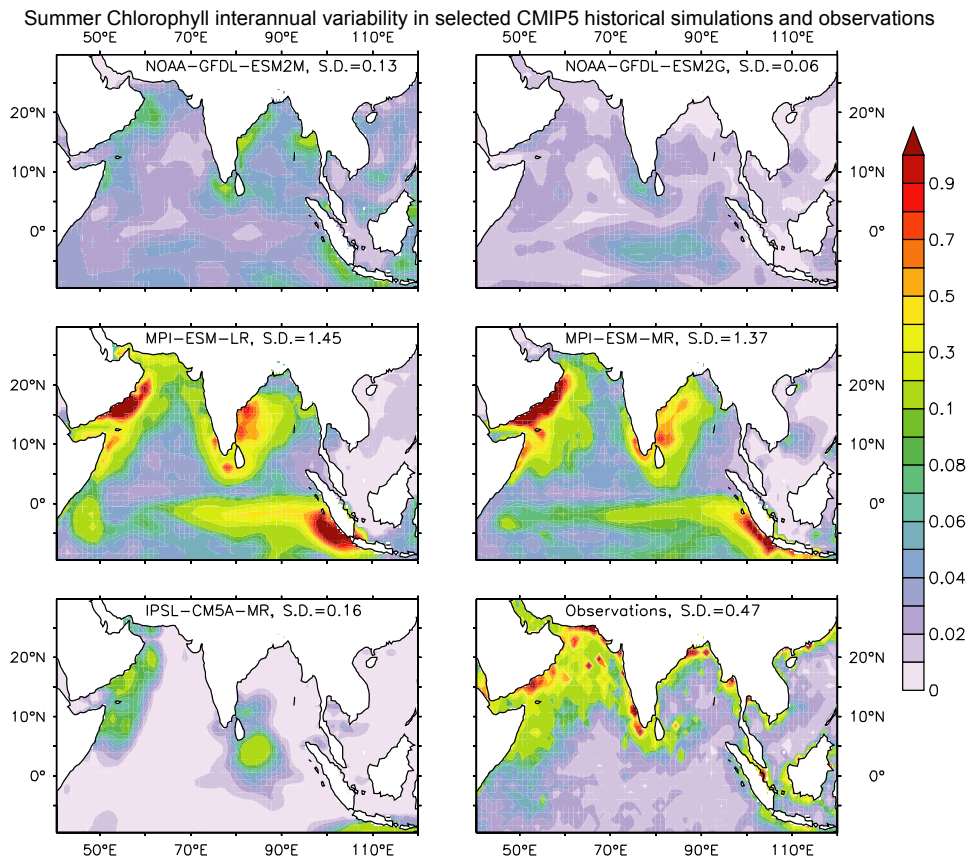


Figure S4. Interannual variability in June-September mean chlorophyll concentration distribution obtained from the selected CMIP5 historical simulations and observations, for the years 1998-2005.

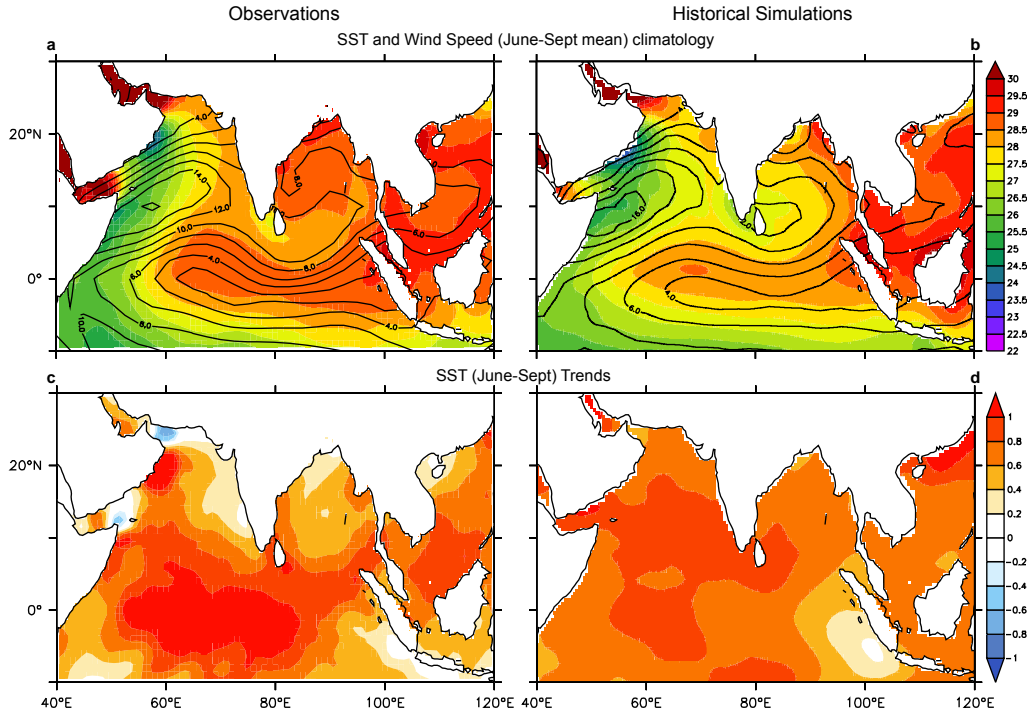


Figure S5. Climatology of June-September (a, b) mean SST (colors, °C) and wind speed (contours, m s^{-1}), and (c, d) SST trends ($^{\circ}\text{C}$ per 56 years), obtained from observations and MPI-ESM-MR historical simulations, for the years 1950-2005. Color shades in c and d denote trends that are significant at 95% confidence levels.

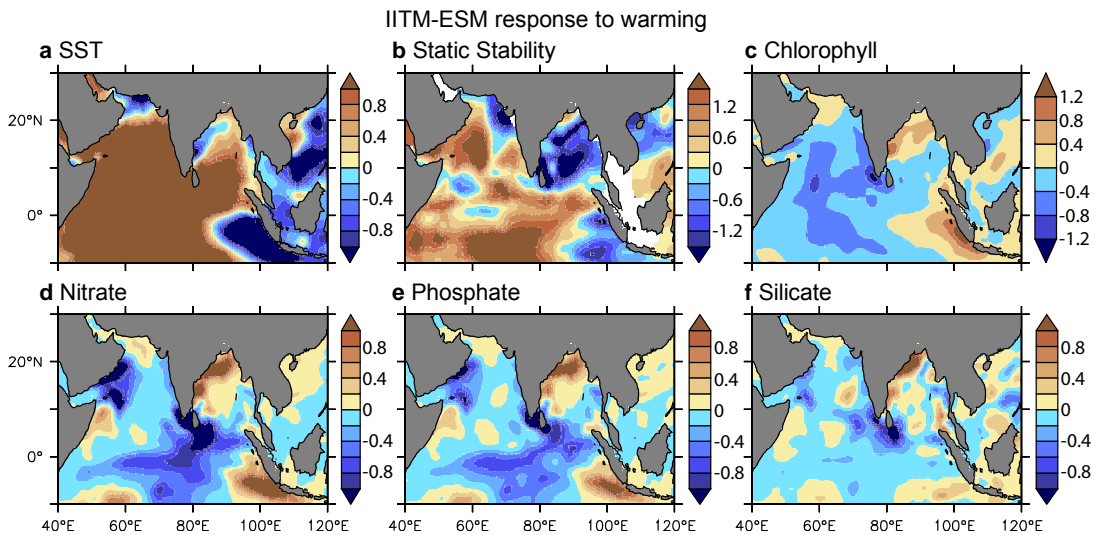


Figure S6. Model simulated (a) SST ($^{\circ}\text{C}$), (b) static stability, (c) chlorophyll (mg m^{-3}), and (d-f) nitrate ($\mu\text{mol L}^{-1}$), phosphate ($10^{-1} \mu\text{mol L}^{-1}$) and silicate ($\mu\text{mol L}^{-1}$) anomalies in response to warming over the Indian Ocean, for June-September. The model simulated anomalies are estimated from the sensitivity run where SST anomalies of the order of 1.5°C is introduced over the western Indian Ocean (CFSv2_{IO}), with respect to a model control run (CFSv2_{CTL}).

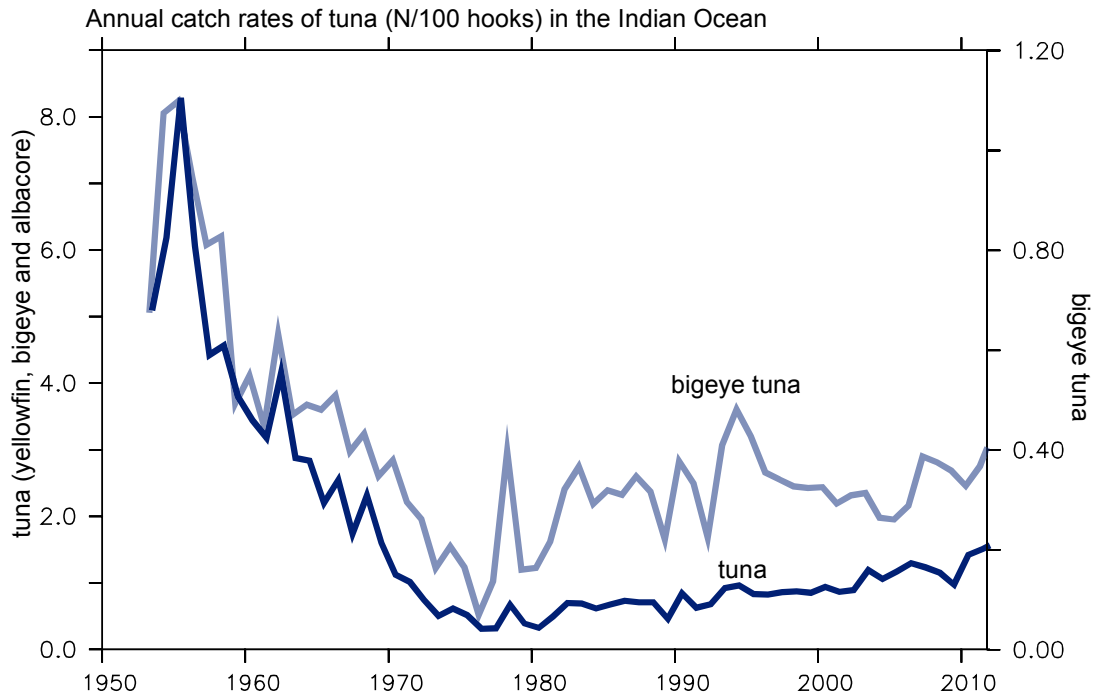


Figure S7. Annual catch rates (N/100 hooks) for the three principle species of tuna which comprises of 75% of all fishery products, caught by Japanese long-liners in the Indian Ocean. Data is obtained from the Indian Ocean Tuna Commission (IOTC).

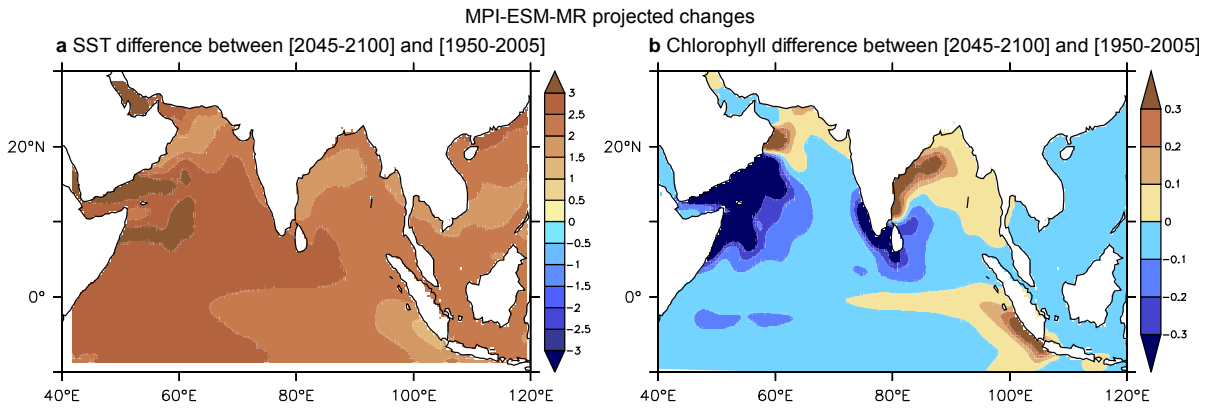


Figure S8. Difference in summer (a) SST ($^{\circ}\text{C}$) and (b) chlorophyll (mg m^{-3}), between future projections (2045-2100) and historical simulations (1950-2005) of MPI-ESM-MR.

#	CMIP5 Model	Atmosphere	Ocean	Ocean BGC	Reference	PCC
1	GISS-E2-H-CC	40 lev, 2.5°/2°	26 lev, 1°/1°	NOBM	<i>Gregg and Casey [2007]</i>	0.21
2	GISS-E2-R-CC	40 lev, 2.5°/2°	32 lev, 1.25°/1°	NOBM	<i>Gregg and Casey [2007]</i>	0.09
3	CESM1-BGC	26 lev, 0.25°/0.94°	60 lev, 1.125°/0.27° -0.53°	BEC	<i>Moore et al. [2004]</i>	0.27
4	CMCC-CESM	39 lev, 3.8°	31 lev, 0.5-2°	PELAGOS	<i>Vichi et al. [2007]</i>	0.39
5	NOAA-GFDL- FSM2M	24 lev, 2.5°/2.0°	50 lev, 0.3-1°	TOPAZ2	<i>Dunne et al. [2013]</i>	0.44
6	NOAA-GFDL- ESM2G	24 lev, 2.5°/2.0°	63 lev, 0.3-1°	TOPAZ2	<i>Dunne et al. [2013]</i>	0.44
7	CanESM2	35 lev, 2.8°/2.8°	40 lev, 1.4°/0.9°	NPZD[<i>Denman and Pena, 1999</i>]	<i>Zahariev et al. [2008]</i>	0.33
8	MRI-ESM1	23 lev.1.125°/1.121	51 lev, 1°/0.5°	NPZD [<i>Oschlies, 2001</i>]	<i>Adachi et al. [2013]</i>	0.06
9	HadGEM2-CC	60 lev, 1.2°/1.9°	40 lev, 1°/0.3-1°	Diat-HadOCC	<i>Palmer and Totterdell [2001]</i>	0.37
10	HadGEM2-ES	38 lev, 1.2°/1.9°	40 lev, 1°/0.3-1°	Diat-HadOCC	<i>Palmer and Totterdell [2001]</i>	0.37
11	MPI-ESM-LR	47 lev, 1.9°	40 lev, 1.5°	HAMOCC5.2	<i>Ilyina et al. [2013]</i>	0.59
12	MPI-ESM-MR	95 lev, 1.9°	40 lev, 0.4°	HAMOCC5.2	<i>Ilyina et al. [2013]</i>	0.50
13	CNRM-CM5	31 lev, 1.4°	42 lev, 1°	PISCES	<i>Séférian et al. [2013]</i>	0.03
14	IPSL-CM5A- MR	39 lev, 1.2°/2.5°	31 lev, 2°/0.5-2°	PISCES	<i>Séférian et al. [2013]</i>	0.48
15	IPSL-CM5B-LR	39 lev, 1.2°/2.5°	31 lev, 2°/0.5-2°	PISCES	<i>Séférian et al. [2013]</i>	0.15
16	IPSL-CM5A-LR	39 lev, 1.9°/3.8°	31 lev, 2°/0.5-2°	PISCES	<i>Séférian et al. [2013]</i>	0.39

Table S1. Details of the CMIP5 models having ocean biogeochemistry (BGC) component, providing historical simulations of chlorophyll concentration. Pattern correlation coefficient (PCC) between climatological summer means of the observations and CMIP5 historical simulations for chlorophyll concentrations during the period 1998-2005 is provided in the last column.

References

- Adachi, Y., S. Yukimoto, M. Deushi, A. Obata, H. Nakano, T. Y. Tanaka, M. Hosaka, T. Sakami, H. Yoshimura, and M. Hirabara (2013), Basic performance of a new earth system model of the Meteorological Research Institute (MRI-ESM1), *Papers in Meteorology and Geophysics*, 64, 1-19.
- Beaulieu, C., S. A. Henson, J. L. Sarmiento, J. P. Dunne, S. C. Doney, R. Rykaczewski, and L. Bopp (2013), Factors challenging our ability to detect long-term trends in ocean chlorophyll, *Biogeosciences*, 10, 2711–2724.
- Behrenfeld, M. J., R. T. O'Malley, D. A. Siegel, C. R. McClain, J. L. Sarmiento, G. C. Feldman, A. J. Milligan, P. G. Falkowski, R. M. Letelier, and E. S. Boss (2006), Climate-driven trends in contemporary ocean productivity, *Nature*, 444(7120), 752-755.
- Boyce, D. G., M. R. Lewis, and B. Worm (2010), Global phytoplankton decline over the past century, *Nature*, 466(7306), 591-596.
- Brewin, R. J., D. E. Raitsos, G. Dall'Olmo, N. Zarokanellos, T. Jackson, M.-F. Racault, E. S. Boss, S. Sathyendranath, B. H. Jones, and I. Hoteit (2015), Regional ocean-colour chlorophyll algorithms for the Red Sea, *Remote Sensing of Environment*, 165, 64-85.
- Denman, K., and M. Pena (1999), A coupled 1-D biological/physical model of the northeast subarctic Pacific Ocean with iron limitation, *Deep Sea Research Part II: Topical Studies in Oceanography*, 46(11), 2877-2908.
- Dunne, J. P., A. Gnanadesikan, J. L. Sarmiento, and R. D. Slater (2010), Technical description of the prototype version (v0) of tracers of phytoplankton with allometric zooplankton (TOPAZ) ocean biogeochemical model as used in the Princeton IFMIP model, *Biogeosciences*, 7, 3593.
- Dunne, J. P., J. G. John, E. Shevliakova, R. J. Stouffer, J. P. Krasting, S. L. Malyshev, P. Milly, L. T. Sentman, A. J. Adcroft, and W. Cooke (2013), GFDL's ESM2 Global Coupled Climate–Carbon Earth System Models. Part II: Carbon System Formulation and Baseline Simulation Characteristics*, *Journal of Climate*, 26(7), 2247-2267.
- Goyet, C., and A. Poisson (1989), New determination of carbonic acid dissociation constants in seawater as a function of temperature and salinity, *Deep Sea Research Part A. Oceanographic Research Papers*, 36(11), 1635-1654.
- Gregg, W. W., and N. W. Casey (2007), Modeling coccolithophores in the global oceans, *Deep Sea Research Part II: Topical Studies in Oceanography*, 54(5), 447-477.
- Henson, S. A., J. L. Sarmiento, J. P. Dunne, L. Bopp, I. D. Lima, S. C. Doney, J. John, and C. Beaulieu (2010), Detection of anthropogenic climate change in satellite records of ocean chlorophyll and productivity, *Biogeosciences*, 7, 621-640.
- Ilyina, T., K. D. Six, J. Segschneider, E. Maier-Reimer, H. Li, and I. Núñez-Riboni (2013), Global ocean biogeochemistry model HAMOCC: Model architecture and performance as component of the MPI-Earth system model in different CMIP5 experimental realizations, *Journal of Advances in Modeling Earth Systems*, 5(2), 287-315.

- Maier-Reimer, E., and K. Hasselmann (1987), Transport and storage of CO₂ in the ocean—an inorganic ocean-circulation carbon cycle model, *Climate dynamics*, 2(2), 63-90.
- McCreary, J., R. Murtugudde, J. Vialard, P. Vinayachandran, J. D. Wiggert, R. R. Hood, D. Shankar, and S. Shetye (2009), Biophysical processes in the Indian Ocean, *Indian Ocean Biogeochemical Processes and Ecological Variability*, 9-32.
- Moore, J. K., S. C. Doney, and K. Lindsay (2004), Upper ocean ecosystem dynamics and iron cycling in a global three-dimensional model, *Global Biogeochemical Cycles*, 18(4).
- Müller, D., H. Krasemann, R. J. Brewin, C. Brockmann, P.-Y. Deschamps, R. Doerffer, N. Fomferra, B. A. Franz, M. G. Grant, and S. B. Groom (2015), The Ocean Colour Climate Change Initiative: I. A methodology for assessing atmospheric correction processors based on in-situ measurements, *Remote Sensing of Environment*, 162, 242-256.
- Narvekar, J., and S. Prasanna Kumar (2014), Mixed layer variability and chlorophyll a biomass in the Bay of Bengal, *Biogeosciences*, 11, 3819-3843.
- Oschlies, A. (2001), Model-derived estimates of new production: New results point towards lower values, *Deep Sea Research Part II: Topical Studies in Oceanography*, 48(10), 2173-2197.
- Palmer, J., and I. Totterdell (2001), Production and export in a global ocean ecosystem model, *Deep Sea Research Part I: Oceanographic Research Papers*, 48(5), 1169-1198.
- Prasanna, V. (2015), Assessment of South Asian Summer Monsoon Simulation in CMIP5-Coupled Climate Models During the Historical Period (1850–2005), *Pure and Applied Geophysics*, 1-24.
- Ravichandran, M., M. Girishkumar, and S. Riser (2012), Observed variability of chlorophyll-a using Argo profiling floats in the southeastern Arabian Sea, *Deep Sea Research Part I: Oceanographic Research Papers*, 65, 15-25.
- Rykaczewski, R. R., and J. P. Dunne (2011), A measured look at ocean chlorophyll trends, *Nature*, 472(7342), E5-E6.
- Ryther, J. H., and C. Yentsch (1957), The estimation of phytoplankton production in the ocean from chlorophyll and light data, *Limnology and oceanography*, 281-286.
- Séférian, R., L. Bopp, M. Gehlen, J. C. Orr, C. Ethé, P. Cadule, O. Aumont, D. S. y Méliá, A. Voltaire, and G. Madec (2013), Skill assessment of three earth system models with common marine biogeochemistry, *Climate Dynamics*, 40(9-10), 2549-2573.
- Swapna, P., M. Roxy, K. Aparna, K. Kulkarni, A. Prajeesh, K. Ashok, R. Krishnan, S. Moorthi, A. Kumar, and B. Goswami (2015), The IITM Earth System Model: Transformation of a Seasonal Prediction Model to a Long Term Climate Model, *Bulletin of the American Meteorological Society*.
- Vichi, M., N. Pinardi, and S. Masina (2007), A generalized model of pelagic biogeochemistry for the global ocean ecosystem. Part I: Theory, *Journal of Marine Systems*, 64(1), 89-109.
- Zahariev, K., J. R. Christian, and K. L. Denman (2008), Preindustrial, historical, and fertilization simulations using a global ocean carbon model with new parameterizations of iron limitation, calcification, and N₂ fixation, *Progress in Oceanography*, 77(1), 56-82.